

# Poly(ethylene glycol) Carbodiimide Coupling Reagents for the Biological and Chemical Functionalization of Water-Soluble Nanoparticles

Hongyan Shen, Ali M. Jawaid, and Preston T. Snee\*

Department of Chemistry, University of Illinois at Chicago, 845 West Taylor Street, Chicago, Illinois 60607-7061

**M**etallic and semiconductor nanoparticles (NPs, or quantum dots) have attracted enormous attention over the past several decades due to their unique size-dependent physical and optical properties. Semiconductor NPs may be luminescent and display narrow and size tunable emission spectra, high quantum yields, and exceptional photostability. Water-solubilized NPs can be functionalized to produce especially useful systems that have found applications in imaging, tracking, sensing, and labeling in biology.<sup>1–10</sup> However, these applications would not exist were it not for the development of water solubilization and chemical and biological conjugation methods for the generally hydrophobic materials that are created using colloidal synthetic procedures. Since the problem with the conversion of the hydrophobic semiconductor NPs into water-soluble systems was first addressed in 1998,<sup>11,12</sup> several methods have been developed to water solubilize NPs.<sup>13</sup> Generally, these methods involve cap exchange or encapsulation. Cap exchange involves stripping the native TOP/TOPO surface ligands and replacing them with bifunctional surfactants such as mercapto acids. Our group and others have found that encapsulation of NPs in amphiphilic polymers is highly robust; the use of a 40% octylamine-modified poly(acrylic acid) polymer is fairly ubiquitous in this regard.<sup>14,15</sup>

The solubilization of NPs in water is unfortunately only half of the problem when synthesizing functional materials—the nanoparticles must further be derivatized with chemical or biological vectors before they serve a useful purpose.<sup>16–19</sup> Water-soluble NPs are often synthesized using sys-

**ABSTRACT** Many types of metal and semiconductor nanoparticles (NPs) are created *via* colloidal synthetic methods, which renders the materials hydrophobic. Such NPs are dispersed in water through surface organic cap exchange or by amphiphilic polymer encapsulation; often, water solubility is achieved *via* the presence of carboxylic acid functionalities on the solubilizing agents. While this renders the material water-soluble, subsequent functionalization of the systems can be very difficult. The most obvious method to derivatize carboxylic acid coated NPs is to conjugate chemical and biological moieties containing amine functionality to the NP surface using the water-soluble activator 1-ethyl-3-(3-dimethylaminopropyl) carbodiimide hydrochloride (EDC). However, the excess use of this reagent appears to cause complete and permanent precipitation of the NPs. We report here our method on the chemical and biological functionalization of a variety of semiconductor nanoparticle systems using novel carbodiimide reagents. These reagents do not cause precipitation even at high loading levels and can be used to efficiently functionalize carboxylic acid coated NPs.

**KEYWORDS:** nanocrystals · quantum dots · amide bonds · carbodiimide coupling · functionalization

tems with carboxylic acid terminated functionality; an obvious solution is to cross-link the organic shell with a primary amine containing chemical or biological vector using a carbodiimide activator such as 1-ethyl-3-(3-dimethylaminopropyl) carbodiimide hydrochloride (EDC). However, quenching caused by the precipitation of carboxylic acid coated NPs by the use of excess EDC has been observed by our group and many others.<sup>1,16,20,21</sup> The NP aggregation can cause the loss of an entire sample if the material is exposed to excess EDC (on the order of  $10^4$  per NP by mole); our work suggests this precipitation is permanent. Herein, we report our efforts on modulating the chemical properties of water-soluble carbodiimide reagents to eliminate precipitation of the NPs. We have synthesized several novel carbodiimide compounds which do not cause precipitation of nanoparticles and can be used to functionalize amphiphilic polymer-coated NPs with very high yield.

\*Address correspondence to sneep@uic.edu.

Received for review December 18, 2008 and accepted March 03, 2009.

Published online March 10, 2009.  
10.1021/nn800870r CCC: \$40.75

© 2009 American Chemical Society

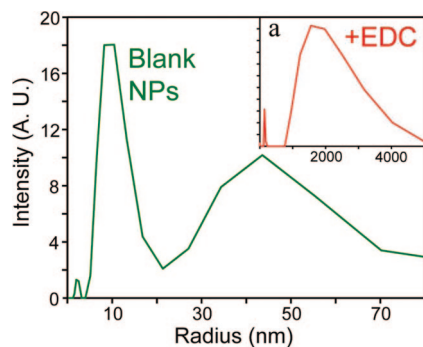


**Figure 1.** Dynamic light scattering characterization of the size of water-soluble CdSe/ZnS NPs. The main peak at  $\sim 10$  nm radius is due to the NPs, while the  $\sim 45$  nm radius is likely from dust particles. Inset a: After exposure to excess EDC ( $\sim 3 \times 10^5$  per NP by mole), the precipitation of the NPs is evident as the average size of the particulates increases to  $\sim 1550$  nm. There is no peak at 10 nm, while the small peak near  $\sim 100$  nm is attributed to small dust particulates. The absorption and emission of the samples before and after EDC precipitation is shown in Figure 2.

## RESULTS AND DISCUSSION

**EDC-Induced NP Precipitation.** Our group and others have noted that the coupling reagent 1-ethyl-3-(3-dimethylaminopropyl) carbodiimide hydrochloride (known as EDC) often results in precipitation of water-solubilized NPs. To demonstrate this effect, we have examined the size distribution of a sample of water-soluble CdSe/ZnS NPs using dynamic light scattering (DLS) before and after exposure to excess EDC. As shown in Figure 1, the NPs initially have a radius of 10 nm (a secondary peak appears at 45 nm, which we attribute to dust particles as confirmed with gel permeation chromatography). After exposure to EDC and incubation overnight, the NPs were clearly precipitated due to their “snowflake” appearance and loss of emission intensity which was verified in the DLS data shown in the inset of Figure 1. The average size increased  $\sim 150$ -fold due to the induced precipitation of the NPs, which can be seen in the absorption spectrum of the sample which is dominated by scattering, as shown in Figure 2.

As a result of the chemical exposure, the emission intensity of the NPs is quenched by 65% relative to the untreated sample. We have also precipitated a sample of CdSe/ZnS NPs using EDC and stored them since March of 2008; none of the material appears to have resolubilized, although it is difficult to imagine that the EDC has not hydrolyzed at the time of this writing (10 months later). Thus, the precipitation appears permanent, which would likely be the case if the amphiphilic NP polymer coating was lost.

**MPEG CD Synthesis.** Many of the current methods to water solubilize hydrophobic colloidal synthesized NPs involve the utilization of systems with carboxylic acid moieties. As such, the derivatization of water-soluble NPs through highly stable amide bonds should be simple and efficient through the use of amine func-

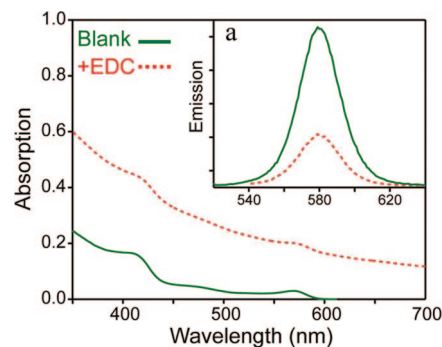


**Figure 2.** Absorption spectra of water-soluble CdSe/ZnS NPs before and after exposure to EDC. The agglomeration characterized from DLS measurements is reflected by the scattering absorption features in the sample after exposure to EDC. Inset a: Fluorescence emission spectra of CdSe/ZnS NPs before and after exposure to EDC reveal that the emission intensity of the NPs is reduced by 65% due to the EDC-induced precipitation. These samples were also characterized by DLS (Figure 1).

tional vectors with a carbodiimide activating agent. While this strategy is often employed, our own survey of the literature has found that EDC is often used sparingly, and many researchers have to refilter their samples after exposure of aqueous NPs to this reagent. As noted by our group and others and demonstrated here, exposure to excess EDC causes complete precipitation of the sample, which in our own observations suggests is permanent. When we began to examine the precipitation of NPs with EDC, our initial hypothesis was that residual amine surfactants, generally used in the synthesis of NPs such as CdSe/ZnS, allow the NPs to cross-link, which is the source of the observed precipitation. We synthesized CdSe/ZnS without the use of amines, at any step, according to some of the original procedures;<sup>22,23</sup> after water solubilizing the NPs using octylamine-modified PAA amphiphilic polymers and purification, we observed severe precipitation of the materials after exposure to excess EDC.

At this point, the chemical reactivity of the carbodiimide seemed less responsible for the observed precipitation as there is no reaction that the EDC could cause that would allow NPs to precipitate in water. We then focused on the water solubilizing moiety of EDC: the terminal cationic *N,N*-dimethylamine functionality. We began to question whether the negative charge of the NPs and the positively charged coupling agent were not in fact responsible for our observations; as such, we began to synthesize nonpolar carbodiimide reagents. To this end, we developed on the original procedure for synthesizing water-soluble carbodiimides where the water solubilizing moiety was neither ionic nor reactive with the carbodiimide functionality. In this regard, poly(ethylene glycol) methyl ether (MPEG) satisfies these requirements. We synthesized two MPEG carbodiimide derivatives of various molecular weights and a bifunctional PEG carbodiimide derivative, as discussed in the Experimental Section, and investigated whether

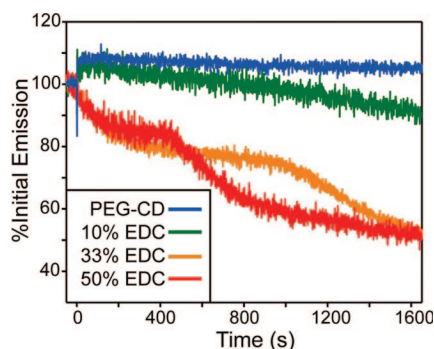


**Figure 3.** Fluorescence intensity of CdSe/ZnS NPs over time after exposure to the carbodiimide reagents discussed in the text compared to the initial emission. Carbodiimide functional poly(ethylene glycol) methyl ether 350 (MPEG 350 CD) was used in this study. The amounts of EDC added to the samples were 10% (green), 33% (orange), and 50% (red) by mole relative to the amount of MPEG 350 CD (blue line,  $1 \times 10^5$  per NP).

these reagents would still precipitate aqueous NP suspensions of various compositions.

**Time-Resolved Precipitation Studies of NPs Exposed to Carbodiimide Reagents.** To study the dynamics of exposure of an aqueous suspension of CdSe/ZnS NPs to the carbodiimides EDC and MPEG 350 CD, we first note that we have demonstrated that precipitation of fluorescent materials reduces the emission intensity. As such, we injected solutions of the carbodiimide reagents EDC and MPEG 350 CD into aqueous CdSe/ZnS NP suspensions while monitoring the fluorescent emission intensity over time. Shown in Figure 3 are the normalized emission intensities after correction for the dilution that occurs after reagent injection. The PEG 350 CD sample ( $1 \times 10^5$  molar excess/NP) shows some CdSe/ZnS brightening; however, this effect is slight and is very likely due to an increase in signal simply from fluorescence waveguiding to the detector *via* dilution. The sample emission intensity remains relatively constant, which indicates the nanoparticles are stable in solution. In a separate experiment, injection of a 10% molar equiv of EDC to MPEG 350 CD into a fresh 3 mL CdSe/ZnS sample of the same concentration causes a similar, slight increase in the CdSe/ZnS signal; however, over time, the emission intensity decreases. When exposed to 33 and 50% molar equiv, there is a clear and immediate loss of emission intensity which we can associate with the precipitation of the NPs. After monitoring the emission, the presence of EDC-induced precipitated NPs was confirmed visually as the sample had a “snowdome”-like appearance under ambient lighting (see Figure S8 of the Supporting Information). Consequently, exposure to high concentrations of neutral MPEG 350 CD does not cause precipitation of the NPs under these conditions nor any other that we have studied, which was confirmed with DLS measurements. Precipitation of NPs was never visually observed when exposing NPs to MPEG 750 CD, as well. The efficacy of using the carbodiimide reagent as an activator for form-

ing amide bonds with NPs and other materials is discussed in the following sections.

It is interesting to note that the EDC precipitation data reveal two correlated, yet distinctly separated, dynamical processes occurring after exposure to the reagent. After addition of EDC, a second-order kinetic drop in NP emission is observed, which is followed up by a second quenching event after some critical time. While it is difficult to know what can cause this type of dynamic, we propose that the initial event is due to multiple EDC molecules associating with the NP amphiphilic polymer coating or perhaps even directly with the trioctylphosphine oxide coated ZnS surface. This also accounts for the clear second-order nature of the dynamic as seen in Figure 3. This interaction may result in a loss of polymer coating such that the local (surface NP associated) concentration of polymers falls below the critical micelle concentration (CMC). A drop below the CMC would explain the sudden initiation of the second event: the mass agglomeration and quenching of CdSe/ZnS NPs as they have lost too many surfactant polymers to remain stable in an aqueous solution. This would also explain the apparent permanent precipitation of NPs caused by EDC as noted previously. We hope to further explore this phenomenon in the near future with EDC and other ions known to precipitate NPs.

**Amide Bond Formation with MPEG CD.** The carbodiimide functionalization of amphiphilic carboxylic acid polymer coated NPs with primary amine functional chemical and biological vectors is a very desirable method. The amide bond is much more stable within biological systems than esters; further, most proteins have primary amine functionality on their surface. As discussed above, there are serious issues with the use of excess commercially available EDC reagent which limits the ability to create highly multifunctional NP systems. Having established that our neutral carbodiimide reagents do not cause NP precipitation, we next examined whether the carbodiimide functionality is effective for activating carboxylic acid groups for amide bond formation.

First, the coupling of 40% octylamine-modified poly(acrylic acid) CdSe/ZnS NPs with an amine functional dye represents an ideal model system as the reaction efficiency is easy to calculate using simple UV/vis spectroscopy; further, the demonstration of energy transfer between properly matched NP fluorescent donor to dye acceptor is a second observable to attest to the conjugation efficiency. To accomplish this, we synthesized 540 nm emitting CdSe/ZnS NPs, which is an ideal donor for 545 nm absorbing TAMRA cadaverine dye. Generally, we started with 1 mL of a stock NP solution, which was consistently exposed to a  $\sim 140$ -fold molar excess of dye with respect to the nanoparticle; optimization of the method was accomplished by varying the amount of MPEG CD reagent used relative to the dye

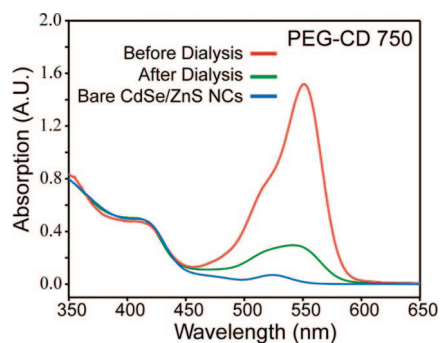


**Figure 4.** Absorption spectra of CdSe/ZnS–TAMRA cadaverine dye before (red line) and after (green line) dialysis using 100K MW cutoff filters. Compared to the bare NPs (blue), there is clearly retention of dye which must be bound to the NP via carbodiimide coupling. This example represents the highest yield that was achieved with the MPEG 750 CD reagent (23%).

and varying the amount of time that the coupling was allowed to occur. The absorption spectra before and after removing the unreacted dye were used to calculate reaction yields as discussed in the Experimental Section. The data for two reagents, MPEG 750 and 350 CD, are shown in Figures 4 and 5.

The first reagent studied was the larger MPEG 750 CD. Initially, we found that a significant excess of this carbodiimide to dye was necessary to observe an appreciable yield. Generally, using a 100-fold excess and stirring overnight gave  $\sim 7\%$  yield; the use of more reagent up to  $300\times$  did not seem to affect the results. Similar efficiency was observed when coupling TAMRA cadaverine to  $\text{Fe}_2\text{O}_3$  NPs as shown in the Supporting Information. Next, we studied the efficiency of coupling the dye to CdSe/ZnS with a 100-fold excess of MPEG 750 CD as a function of time, where we found that stirring for 3 days gave the highest observed yield (23%). The data from this sample are shown in Figure 4. We were surprised to see that the reagent was active for so long after exposure to water, which led us to believe that the length of the MPEG moiety was “protecting” the carbodiimide function from water and perhaps from reacting with the NP polymer surface. This led to

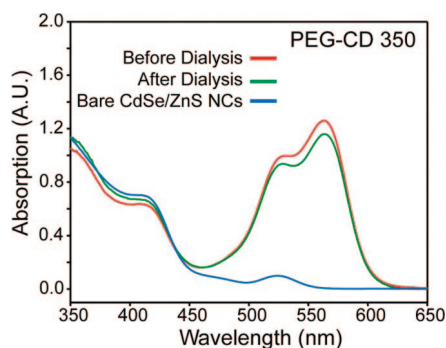


**Figure 5.** Absorption spectra of CdSe/ZnS and TAMRA dye before (red line) and after (green line) dialysis using 100K MW cutoff filters. This example represents the highest yield that was achieved with the MPEG 350 CD reagent (93%), which was a significant improvement compared to the best results using MPEG 750 CD (Figure 4).

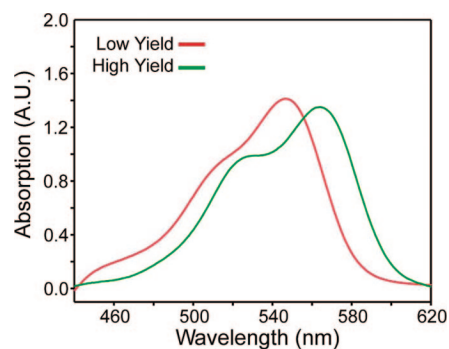


**Figure 6.** Normalized absorption spectra of TAMRA dyes bound to CdSe/ZnS NPs after subtraction of the CdSe/ZnS component. Data are taken from a sample with  $\sim 33$  dyes/NP (green) and  $\sim 130$  dyes/NP (red). Clearly, the higher loading levels have affected the dye’s photophysical properties. The 33:1 conjugate was prepared with MPEG 750 CD, and the 130:1 loaded sample was prepared with MPEG 350 CD.

the conclusion that the polymer functionality of MPEG 750 CD is too long and suppresses amide bond formation. As such, we synthesized and studied a much smaller reagent with a shorter PEG functionality, MPEG 350 CD.

Our initial results with MPEG 350 CD clearly demonstrated that this was a highly effective reagent for coupling amine functional dyes to amphiphilic polymer-coated NPs. First, it was found that the optimum MPEG 350 CD to dye ratio was  $230\times$ , over twice that observed with the larger MPEG carbodiimide. The efficiencies were substantially improved as well with a 93% coupling yield using a  $230\times$  excess reagent as evident from the data in Figure 5; in fact, we did not perform time-dependent experiments as they did not seem necessary. This led us to conclude that steric hindrances lowered the reaction yields observed with the MPEG 750 CD reagent. Another interesting observation was made at this point; the dye spectra appeared to red shift with increasing reaction yield. The spectra of the dye in two constructs, with dye to NP ratios of 33:1 and another with 130:1, reveal that the absorption of the dye has been noticeably altered in the shape and absorption maximum as shown in Figure 6. Perhaps the dye is being encapsulated within the interior of the polymer in the high loading conditions, which can change the absorptive properties of the dye.<sup>18</sup> We also speculate whether the dyes begin to associate with one another at very high loading concentrations, which would likely red shift their absorptions.

The particular CdSe/ZnS NP and dye were chosen such that they may undergo fluorescent resonant energy transfer (FRET)<sup>24</sup> from the NP donor to the TAMRA dye acceptor. While the emission spectra show suppressed NP emission with concomitant enhanced dye emission, we discovered that energy transfer is clearly visible to the eye, as shown in Figure 7. Not only can the presence of the dye be observed from the increase of the pink color as more MPEG 350 CD was used in the synthesis of the coupled construct, the emission from



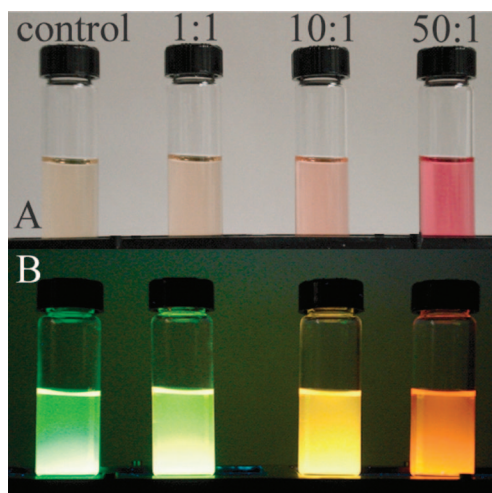


**Figure 7.** (A) Visible light image of CdSe/ZnS NP samples after coupling to amine functional TAMRA dye as a function of the MPEG 350 CD to dye ratio. (B) Emission under UV light excitation of the same samples. A significant amount of dye is coupled using a  $\sim$ 50:1 ratio of carbodiimide reagent to dye as evident from energy transfer from the NP to the emissive dye.

the TAMRA dye becomes dominant as the loading levels of dye were increased as confirmed with fluorometry. Next, we investigated the synthesis of chemically sensitive functional NPs by the coupling of a CdS/ZnS NP donor to a pH-sensitive amine functional fluorescein dye acceptor. As shown in Figure 8, the system displays a ratiometric response to pH most likely due to the variation of FRET efficiencies due to the change in the local chemical environment, as has been reported earlier.<sup>8,16</sup> Consequently, we have found that MPEG CD is a versatile reagent and can be used to derivatize several NP systems to create a variety of functional materials. On a last note, we found that using a bifunctional carbodiimide PEG reagent caused NP precipitation; however, this was likely due to the activation of carboxylic acid functionalities on separate NPs with the same reagent. Addition of excess base resolubilized the NPs; however, we did not study this system further.

While the conjugation of NPs and dyes was used to optimize the procedure for MPEG CD coupling conditions, most research involving NPs revolves around bio-

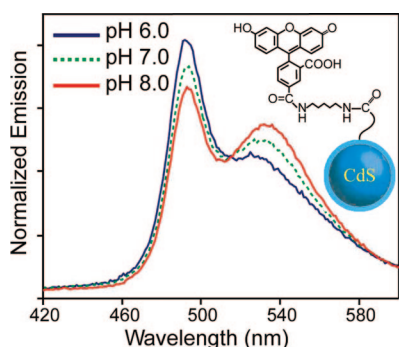


**Figure 8.** Emission spectra of a CdS/ZnS–fluorescein cadaverine dye conjugate as a function of pH. Inset shows a scheme of the coupled construct.

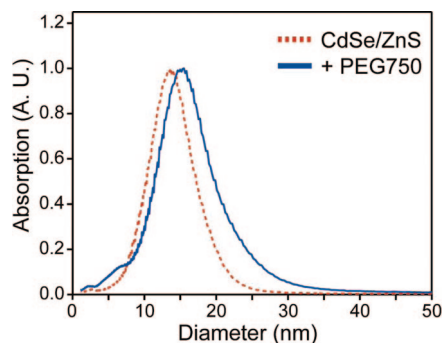


**Figure 9.** Gel permeation chromatography trace of aqueous CdSe/ZnS NPs and amine functional MPEG 750/NP conjugate. The increase in size is indicative of the coating of the NPs with the poly(ethylene glycol) methyl ether.

logical imaging. To this end, the synthesis of biologically compatible materials is most important, and as such we examined two relevant systems. First, poly(ethylene glycol) coating of NPs will decrease nonspecific adsorption of proteins in biological systems and may prevent precipitation due to high salt concentrations or changes in pH.<sup>25–27</sup> As we had already synthesized a quantity of the amine derivative of poly(ethylene glycol) methyl ether (MW 750) for this study, we examined whether the carbodiimide functional MPEG 350 CD was effective for PEGylation of amphiphilic PAA polymer encapsulated CdSe/ZnS NPs. Following the optimized procedures for the use of MPEG 350 CD, we attempted to conjugate as many as  $\sim$ 1000 MPEGs per NP. Unfortunately, it is difficult to estimate the reaction yield in this system; however, we did verify the presence of MPEG 750 on the surface of the NPs *via* analysis with GPC as shown in Figure 9. The PEGylated NPs were found to have an increase in diameter from 13.7 nm for the unfunctionalized blank NPs to 15.2 nm for the PEGylated NPs. Further, the PEGylated NPs were found to be more resistant to precipitation by salts such as calcium chloride. Consequently, the MPEG 350 CD reagent is effective for the coating of NPs with more than just amine functional dyes; however, we do not know the reaction yield at present.

The synthesis of NP/protein conjugates is very important for using nanoparticles to image biological systems. As such, we investigated the conjugation of CdSe/ZnS NPs with excess streptavidin under various protein to NP ratios. During the initial phase of this study, we examined the coupling of aqueous solutions of NPs with low streptavidin to NP ratios (1 $\rightarrow$ 5 $\times$ ) using MPEG 350 CD. After stirring overnight and subsequent dialysis, we found that a large amount of material was precipitating. As avoiding NP losses was the purpose of this study and our previous work demonstrated that MPEG 350 CD is safe to use in this regard, we began to examine whether the tetrameric nature of streptavidin was at fault—essentially, whether the protein was cross-linking NPs together. Analysis with GPC confirmed that the majority of our materials eluted within the dead vol-

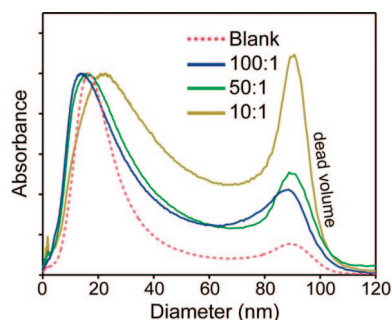


**Figure 10.** Gel permeation chromatography traces of aqueous CdSe/ZnS NPs and streptavidin conjugate as a function of the streptavidin to NP ratio used during the synthesis. The data are normalized to the unaggregated peak near 20 nm diameter. Clearly, a large excess of protein is needed to prevent agglomeration as evident by the increase in the dead volume peak as the protein to NP ratio is lowered.

ume (>90 nm diameter), which suggested that the NPs were highly cross-linked. In the next round of optimization, we heavily increased the streptavidin to NP ratio from 10:1, 50:1, and 100:1 and repeated the coupling using excess PEG 350 CD. No precipitation observed and analysis with GPC under these conditions revealed that the formation of large aggregates was suppressed at high (100:1) streptavidin to NP loading ratios. As shown in Figure 10, the highest protein loading has the smallest peak in the dead volume, which increased as the loading ratio became smaller. After dialysis and measuring the UV/vis spectra of the streptavidin and blank NPs, we determined that  $\sim 2$  proteins were conjugated to every NP (see Supporting Information). While this may seem to reveal a low efficiency, it is unlikely that 100 proteins could be coupled to a single NP; as such, the excess protein simply blocks the formation of  $(-NP-streptavidin)_x$  aggregates.

After a method of preventing the precipitation of the NPs during the coupling of the protein was developed, we next examined how to verify the activity of streptavidin on the surface of the nanoparticles *via* their interaction with biotin. We developed an inexpensive assay by measuring the emission of a solution of functionalized NPs that was passed through cellulose and biotinylated cellulose columns. A control sample was made by diluting the original solution into the same volume as the effluent from the columns and comparing the fluorescence under identical conditions. As shown in Figure 11, there is some loss of emission intensity when streptavidin coupled CdSe/ZnS NPs are run through the cellulose control column, which is likely due to nonspecific adsorption to the cellulose. However, when run through an identical column containing biotinylated cellulose, there is no emission from the effluent and a bright orange (CdSe/ZnS) band was observed at the very top of the column. Consequently, the MPEG 350 CD coupling of the protein to the NP appears to not have adversely affected the binding of the protein toward biotin.

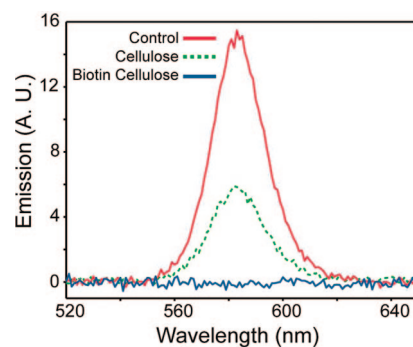


**Figure 11.** Emission of CdSe/ZnS-streptavidin conjugates: this sample was prepared using a 100-fold excess of protein to NP. The control sample was made by diluting the NP-protein constructs to the same volume as the effluent collected. Less emission is observed from NP-protein conjugates after running through a cellulose column, most likely due to nonspecific adsorption; however, no emission is observed if the column contains biotin.

## CONCLUSION

The derivatization of nanoscopic material systems is an active area of research. Some of the synthetic methods developed to create chemical and biological functional NP systems include prereaction of the NP water solubilizing polymers,<sup>18</sup> water solubilizing NPs using amphiphilic polymer backbones with built in chemical handles,<sup>16</sup> formation of disulfide bonds,<sup>17</sup> or by electrostatically conjugating systems through salt bridges.<sup>1</sup> While these methods have proved effective, they generally require a level of synthetic expertise which may be difficult to reproduce for researchers relying on commercially available water-soluble NPs. Fixing the problems with precipitation using commercially available carbodiimide coupling reagents is thus a significant step in this regard, especially as carbodiimide coupling of carboxylic acid and primary amine groups to form stable amide bonds is a well-established protocol.

In the present report, we have shown that NP precipitation and quenching problems associated with the use of the ubiquitous coupling reagent EDC is not due to the carbodiimide functionality; rather, it is due to the net positive charge of the chemical. There are some interesting dynamics observed in the precipitation of NPs caused by EDC, which suggests that the NPs are stripped of their polymer coating causing them to permanently precipitate from solution. Replacement of the *N,N*-dimethylamine functionality of EDC with poly(ethylene glycol) methyl ether creates a carbodiimide coupling reagent which is highly effective and does not cause NP aqueous suspensions to precipitate. This reagent can create a variety of interesting functional systems, including magnetic and emissive NPs, fluorescent chemical sensors, and biologically tailored CdSe/ZnS nanoparticles, in high yield. Further, the reagent can be synthesized in two steps using commercially available amine functional poly(ethylene glycol) methyl ether.

## EXPERIMENTAL SECTION

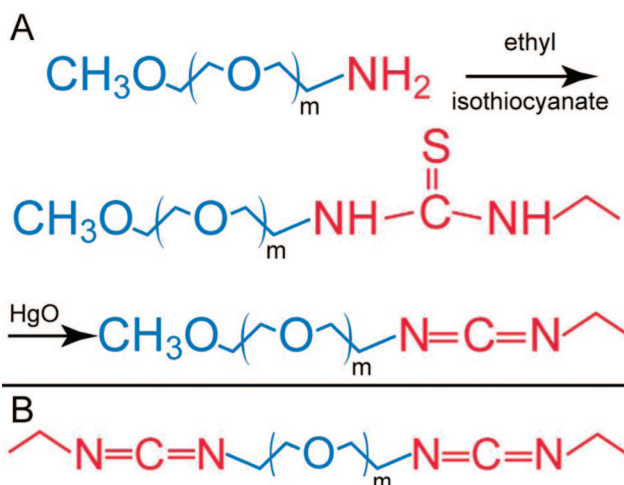
**Materials.** Dyes such as fluorescein-5-carboxamide cadaverine and tetramethylrhodamine-5-carboxamide cadaverine were purchased from Anaspec (San Jose, CA); streptavidin was purchased from the same source. Poly(acrylic acid) (1800 MW), octylamine, biotin, cellulose, thionyl chloride, sodium azide, triphenylphosphine, and solvents were purchased from Sigma-Aldrich (St. Louis, MO). The water-soluble carbodiimide 1-ethyl-3-(3-dimethylaminopropyl) carbodiimide hydrochloride (EDC) was purchased from Advanced Chemtech (Louisville, KY). Concentrated hydrochloric acid and sodium hydroxide were purchased from Fisher Scientific (Pittsburgh, PA). The majority of chemicals were used as received.

As nanoparticle synthesis has become a general practice among many groups, we will note that the methods reported in refs 22 and 28–31 can serve as guides for researchers that are not familiar with these procedures. These methods were used to create CdSe/ZnS, CdS/ZnS, and Fe<sub>2</sub>O<sub>3</sub> nanoparticles exactly as described in the references.

**Octylamine-Modified Polyacrylic Acid.** Many groups who use amphiphilic polymer encapsulation as a method to impart water solubility to hydrophobic NPs employ a system composed of 40% octylamine-modified poly(acrylic acid) (PAA). First, 5.0 g (70 mmol) of commercially available 1800 MW dry PAA powder was diluted into ~70 mL of dry *N,N*-dimethylformamide (DMF). Next, 5.325 g (28 mmol) of EDC was dissolved into the same solution, stirring for 0.5 h followed by the addition of 4.6 mL (28 mmol) of octylamine. The solution was stirred at room temperature overnight before reduction of the solvent under vacuum. Next, distilled water was added to precipitate the polymer which was subsequently isolated by centrifugation; the excess water was discarded. Next, an aqueous sodium hydroxide solution of ~1.7 g (42.5 mmol) of NaOH in 40 mL of H<sub>2</sub>O was added, and the solution was shaken overnight to resolubilize the polymer in water. The crude modified solution was washed by ethyl acetate (3 × 20 mL), which can improve the clarity of the aqueous polymer suspension substantially, especially when using a RAFT synthesized PAA backbone.<sup>16,32</sup> A dilute solution of HCl was added to the aqueous layer until the pH was below 5 to precipitate the polymer again. The solid product was collected by centrifugation and dried under vacuum. The product was slowly and carefully neutralized using a 0.1 M NaOH solution and lyophilized for storage and subsequent use.

**Nanoparticle Water Solubilization.** The nanoparticles used in this study are all initially hydrophobic; as such, we used an amphiphilic polymer coating to render them water-soluble. First, the NPs in growth solution were precipitated with the addition of a few drops of isopropyl alcohol and excess methanol inside of a preweighed glass vial. Materials synthesized in 1-octadecene required more isopropyl alcohol. The flocculate was centrifuged, and the supernatant was removed. The precipitation was performed again for some samples by redispersing the NPs in hexanes followed by isopropyl and methyl alcohol addition followed by centrifugation and vacuum drying. Some NPs become soluble in alcohol solution after one precipitation; these samples were dried after the first isolation step. Generally, we collect ~10 mg of bare NPs to which 50 mg of amphiphilic PAA polymers was added with 5 mL of chloroform and two to three drops of methanol. The mixture was sonicated until the polymer solubilized. After being dried under vacuum, the sample was dissolved in basic water (pH 8–10) to often form clear aqueous solution of NPs. However, some samples of CdSe/ZnS and all iron oxide NPs require additional cleaning through 0.1 μm filters. Dialysis was then performed using 100K molecular weight cutoff filters from Millipore (Amicon Ultra 15, cat. UFC910024). We have found that using smaller molecular weight cutoff filters results in some uncoupled polymer remaining in solution. The solutions were dialyzed with deionized water which tends to be somewhat acidic (pH ~6).

**Synthesis of Poly(ethylene glycol) Methyl Ether Amine (MPEG 350 Amine).** The synthesis of MPEG 350 amine is the first step in the synthesis of the carbodiimide functional material. Unfortunately, the purchase of amine functional poly(ethylene glycol) methyl ether is highly cost prohibitive; as such, we used a recently reported procedure to synthesize the material. The methods re-



**Scheme 1.** (A) Synthetic method employed to synthesize carbodiimide functional poly(ethylene glycol) methyl ether (MPEG CD). (B) Structure of the bifunctional PEG carbodiimide.

ported herein are based on ref 25, although we will repeat them here for completeness. Neat poly(ethylene glycol) methyl ether, average MW 350 g/mol (10 g, 28.6 mmol), was degassed and stirred at 80 °C for 1 h to remove traces of water. The reaction solution was purged with N<sub>2</sub> and cooled in an ice bath before 3.0 mL (41 mmol) of thionyl chloride was added dropwise. The solution was warmed to room temperature and stirred for 2 h to convert the hydroxide group to chloride. Thionyl chloride was removed under vacuum; the pressure of the vacuum system was monitored to ensure removal of the excess reagent. The product was then diluted with 10.0 mL of DMF, and the solvent was removed again under reduced pressure at room temperature to aid in the removal of residual trace amounts of thionyl chloride. Addition and removal of DMF was repeated three times total, which took ~4 days. Next, 75 mL of DMF together with 2.83 g (43.5 mmol) sodium azide was added and stirred overnight at 85 °C with aluminum foil coating the flask to protect the material from light. (Warning: sodium azide is a highly toxic contact explosive.) The DMF was reduced under vacuum before 60 mL of dichloromethane (DCM) was added. A solid precipitate was removed with a glass fritted filter or by centrifugation. The DCM was then removed with vacuum to yield the intermediate azide. The sample was dissolved in 90 mL of tetrahydrofuran (THF), and 8.26 g (31.5 mmol) of triphenylphosphine was added and stirred at room temperature for 4 h before 1.2 mL of water was added and continued stirring for another day. After THF was removed, 200 mL of water was added. The resulting solution was washed with excess toluene twice and was subsequently dried and removed under vacuum to yield a yellow oil. Samples were analyzed using NMR and mass spectrometry; see the Supporting Information. Two other amine functional reagents were synthesized, including a methyl ether MPEG with a molecular weight of 750 and a bifunctional amine starting from poly(ethylene glycol) with a molecular weight of 400. These materials are stored at 4 °C in an airtight container. Despite these precautions, hydrolysis of the product is observed after several months of storage, which is not unexpected given the reactivity of the carbodiimide functionality.

**Carbodiimide Functional Poly(ethylene glycol) Methyl Ether (MPEG 350 CD).** We synthesized two forms of neutral carbodiimide reagents starting with amine functional poly(ethylene glycol) methyl ether with molecular weights of 350 and 750 as outlined in Scheme 1. Another bifunctional carbodiimide was created starting with bisamine poly(ethylene glycol). The methods reported herein are based in part according to the synthesis of EDC first reported by Sheehan *et al.* in ref 33. Approximately 3 g (8.6 mmol) of amine functionalized MPEG 350 was dried under vacuum in a septum-sealed round-bottom flask. Next, the sample was dissolved into 5 mL of anhydrous DMF after which an excess of ethyl isothiocyanate (~1.1 mL, 12.6 mmol) was dripped into the MPEG amine solution slowly with a syringe while stirring. The re-



action was allowed to continue overnight. The next day the DMF was removed under vacuum after which a suspension of 4.65 g (21.5 mmol) of HgO (yellow) in 10 mL of dichloromethane was added. After stirring again overnight, an additional 1.0 g of HgO was added and the solution was again allowed to stir overnight. The yellow mercuric oxide turns green due to HgS formation after which the majority of the byproduct was removed with centrifugation. Some samples appeared to react slowly with the HgO; in these cases, the samples were filtered and recharged with an additional 1.0 g of HgO in DCM and stirred overnight. This process was repeated until no more dark green byproducts were observed. To purify the materials, the MPEG CD can be dissolved into cold ether, which causes the HgS to precipitate. In a few cases, a residual dark green color was observed, which was removed by dissolving the product in water and removing a green insoluble material with centrifugation and filtration. The excess water was then removed immediately under vacuum at room temperature to prevent the hydrolysis of the carbodiimide functionality. The samples may also be purified by flash chromatography over alumina using methanol as the mobile phase. Reaction yields are typically on the order of 90%.

**Biotinylated Cellulose.** To confirm the activity of the protein in streptavidin-coated NPs (see below), these systems were examined by chromatography through a biotinylated cellulose column. The synthesis of biotinylated cellulose was performed according to ref 34. This material was analyzed using NMR spectroscopy; see the Supporting Information.

**Nanoparticle Functionalization.** Several functional materials were synthesized in the course of this study; we will present the most pertinent examples here. Most of the research on PEG CD was conducted to optimize the reaction yield between amphiphilic polymer-coated NPs in water and amine functional materials. For convenience, we chose to synthesize CdSe/ZnS–tetramethylrhodamine-5-carboxamide (TAMRA) cadaverine conjugates as the optical characterization of NP–dye coupling is highly robust. We also investigated the coupling of other dyes, amine functional MPEG and streptavidin.

During the course of our work on CdSe/ZnS NP–TAMRA dye coupling, we developed a scheme that has a 93% reaction yield, which is reported here. A 1 mL quantity of aqueous solution of  $1.38 \times 10^{-6}$  M 540 nm emitting CdSe/ZnS suspensions in slightly acidic (pH ~6) DI water was transferred to a clean glass vial. Next, 11.4 mg of MPEG 350 CD was added to the sample, which was stirred for 0.5 h. Next, 20  $\mu$ L of a 1 mL DMF solution containing 5 mg of tetramethylrhodamine-5-carboxamide cadaverine (194 nmol, approximately 140 $\times$  excess relative to the NPs) was added, and the solution was basified by adding 3 mL of a pH 8 NaOH solution—buffer was not used as the purpose of this study was to examine coupling reactions under conditions with few electrolytes. The solutions were then stirred overnight and were subsequently purified using dialysis centrifuge filters. The amount of MPEG 350 CD reagent was approximately 230 $\times$  excess relative to the dye. The amount and identity of PEG CD reagents to dye ratio was varied and optimized over the course of this work, with this method resulting in the highest yields.

Once we had optimized the procedure for conjugating amine functional dyes to NPs, we also examined the coupling to proteins. To 0.768 mL of a  $6.3 \times 10^{-7}$  M solution of 580 nm emitting CdSe/ZnS NPs was added 0.1891 g of a 0.048 M solution of MPEG 350 CD in DI water. After stirring 0.5 h, 5 mg of streptavidin was diluted into 0.8 mL of a pH 8 NaOH solution from which 0.4 mL was added and stirred overnight; excess material was removed with a 100K MW centrifuge filter the next day. Other loading ratios of streptavidin to NPs were investigated as discussed below. The targeted ratios in this experiment were 100 $\times$  excess of streptavidin proteins per NP, with a 200 $\times$  excess of MPEG 350 CD to the moles of streptavidin.

**Optical Characterization: Reaction Yields.** Absorption spectroscopy was used to determine the reaction yields for creating CdSe/ZnS NP/dye conjugates. After stirring a solution of NPs, PEG CD reagents, and TAMRA–cadaverine dye overnight, the absorption spectrum of a known portion of the solution was measured using a Cary 400 UV/vis. Next, excess dye was removed using 100K MW cutoff centrifuge dialysis filters from Millipore until no dye was observed from the liquid effusate. The UV/vis absorption

spectrum was then measured from the purified sample. As the concentrations of NPs in the first and second measurements were recorded, the absorption spectra from the solution before and after dialysis were normalized by their NP concentrations and plotted together. The NP blank spectrum (also normalized by concentration) is then directly subtracted from each spectrum leaving dye-only absorption features. The yield of reaction is then calculated as the integrated dye absorption after dialysis divided by the integrated absorption before dialysis.

**Optical Characterization: EDC Precipitation.** To demonstrate the effect of excess EDC on NPs, a blank  $6.1 \times 10^{-8}$  M sample (3 mL, 0.18 nmol) of water-soluble CdSe/ZnS NPs was characterized with dynamic light scattering (DLS) and gel permeation chromatography (GPC). Next, the sample was incubated with 10 mg (52  $\mu$ mol) of EDC overnight; the next day the sample sizes were re-characterized with DLS as the aggregates that formed overnight were too large to be characterized with GPC. DLS measurements were also made on MPEG CD 350 exposed CdSe/ZnS samples, which revealed no agglomeration of the NPs. The absorption and emission of these samples were also characterized. Once this work demonstrated that EDC causes precipitation that can be characterized *via* fluorescence quenching, we next explored the dynamics of this process as discussed below.

First, 3 mL of a  $1.5 \times 10^{-7}$  M solution (0.45 nmol) of CdSe/ZnS NPs was placed in a vial inside the optical cavity of a Fluorolog-3 (Horiba Jobin-Yvon) while continuously stirring. The emission of the NPs was monitored at the fluorescence maximum when a 1 mL solution of 0.048 M (48  $\mu$ mol) MPEG 350 CD in deionized water was swiftly injected. This procedure was repeated with fresh NP solutions being exposed to 1 mL of 0.0047, 0.014, and 0.024 M (4.7, 14, and 24  $\mu$ mol) EDC solutions in deionized water. The emission of the NPs was monitored in kinetic mode for ~90 min with a 1 s integration time. The fluorescence data were corrected for the dilution of the NPs after the injection by dividing the signal by the dilution factor. Accurate dilution factors were calculated from the mass of the sample before and after the injection of the carbodiimide solutions.

**Biological Conjugate Characterization.** To verify the activity of the streptavidin conjugates, we examined the retention of these materials on a biotinylated cellulose column. Approximately 2 g of cellulose and biotinylated cellulose was mixed with pH 8 phosphate buffered water and loaded into a small pipet plugged with glass wool. Phosphate buffer was passed through the column until the packing material settled. Next, blank and streptavidin-coupled CdSe/ZnS NPs of known emission intensity were injected into the column from which several milliliters of effusate were collected. Next, the emission of the effluent was measured and normalized for the dilution that occurs as a result of running through the column. All streptavidin-coupled samples were run through the biotinylated column; the 100:1 streptavidin to NP sample was also analyzed through a pure cellulose column to measure nonspecific adsorption losses. The NP–protein conjugates were also studied using gel permeation chromatography in a GE Healthcare Ätka Prime FPLC using pH 8 phosphate buffered water through a Superose 6 10/300 GL column.

**Acknowledgment.** We thank the University of Illinois at Chicago for financial support as well as support from Motorola *via* the University of Illinois Manufacturing Research Center. Also, we thank Wenhao Liu for helpful discussions on the synthesis of amine functional poly(ethylene glycol) methyl ether.

**Supporting Information Available:** NMR and mass spectra of poly(ethylene glycol) coupling reagents and intermediates, absorption and emission data on Fe<sub>2</sub>O<sub>3</sub>–TAMRA dye conjugates, absorption of CdSe/ZnS NP–streptavidin conjugates, and the NMR spectra of biotinylated cellulose. This material is available free of charge *via* the Internet at <http://pubs.acs.org>.

## REFERENCES AND NOTES

- Mattoussi, H.; Mauro, J. M.; Goldman, E. R.; Anderson, G. P.; Sundar, V. C.; Mikulec, F. V.; Bawendi, M. G. Self-Assembly of CdSe–ZnS Quantum Dot Bioconjugates Using an Engineered Recombinant Protein. *J. Am. Chem. Soc.* **2000**, *122*, 12142–12150.



- Willard, D. M.; Carillo, L. L.; Jung, J.; Van Orden, A. CdSe–ZnS Quantum Dots as Resonance Energy Transfer Donors in a Model Protein–Protein Binding Assay. *Nano Lett.* **2001**, *1*, 469–474.
- Dubertret, B.; Skourides, P.; Norris, D. J.; Noireaux, V.; Brivanlou, A. H.; Libchaber, A. *In Vivo* Imaging of Quantum Dots Encapsulated in Phospholipid Micelles. *Science* **2002**, *298*, 1759–1762.
- West, J. L.; Halas, N. J. Engineered Nanomaterials for Biophotonics Applications: Improving Sensing, Imaging, and Therapeutics. *Annu. Rev. Biomed. Eng.* **2003**, *5*, 285–292.
- Cang, H.; Xu, C. S.; Montiel, D.; Yang, H. Guiding a Confocal Microscope by Single Fluorescent Nanoparticles. *Opt. Lett.* **2007**, *32*, 2729–2731.
- Cang, H.; Wong, C. M.; Xu, C. S.; Rizvi, A. H.; Yang, H. Confocal Three Dimensional Tracking of a Single Nanoparticle with Concurrent Spectroscopic Readouts. *App. Phys. Lett.* **2006**, *88*, 223901.
- Howarth, M.; Takao, K.; Hayashi, Y.; Ting, A. Y. Targeting Quantum Dots to Surface Proteins in Living Cells with Biotin Ligase. *Proc. Natl. Acad. Sci. U.S.A.* **2005**, *102*, 7583–7588.
- Snee, P. T.; Somers, R. C.; Nair, G.; Zimmer, J. P.; Bawendi, M. G.; Nocera, D. G. A Ratiometric CdSe/ZnS Nanocrystal pH Sensor. *J. Am. Chem. Soc.* **2006**, *128*, 13320–13321.
- Yezhelyev, M. V.; Qi, L.; O'Regan, R. M.; Nie, S.; Gao, X. Proton-Sponge Coated Quantum Dots for siRNA Delivery and Intracellular Imaging. *J. Am. Chem. Soc.* **2008**, *130*, 9006–9012.
- Rajan, S. S.; Liu, H. Y.; Vu, T. Q. Ligand-Bound Quantum Dot Probes for Studying the Molecular Scale Dynamics of Receptor Endocytic Trafficking in Live Cells. *ACS Nano* **2008**, *2*, 1153–1166.
- Bruchez, M.; Moronne, M.; Gin, P.; Weiss, S.; Alivisatos, A. P. Semiconductor Nanocrystals as Fluorescent Biological Labels. *Science* **1998**, *281*, 2013–2016.
- Chan, W. C. W.; Nie, S. M. Quantum Dot Bioconjugates for Ultrasensitive Nonisotopic Detection. *Science* **1998**, *281*, 2016–2018.
- Michalet, X.; Pinaud, F. F.; Bentolila, L. A.; Tsay, J. M.; Doose, S.; Li, J. J.; Sundaresan, G.; Wu, A. M.; Gambhir, S. S.; Weiss, S. Quantum Dots for Live Cells, *In Vivo* Imaging, and Diagnostics. *Science* **2005**, *307*, 538–544.
- Pellegrino, T.; Manna, L.; Kudera, S.; Liedl, T.; Koktysh, D.; Rogach, A. L.; Keller, S.; Radler, J.; Natile, G.; Parak, W. J. Hydrophobic Nanocrystals Coated with an Amphiphilic Polymer Shell: A General Route to Water Soluble Nanocrystals. *Nano Lett.* **2004**, *4*, 703–707.
- Wu, X. Y.; Liu, H. J.; Liu, J. Q.; Haley, K. N.; Treadway, J. A.; Larson, J. P.; Ge, N. F.; Peale, F.; Bruchez, M. P. Immunofluorescent Labeling of Cancer Marker Her2 and Other Cellular Targets with Semiconductor Quantum Dots. *Nat. Biotechnol.* **2003**, *21*, 41–46.
- Chen, Y.; Thakar, R.; Snee, P. T. Imparting Nanoparticle Function with Size-Controlled Amphiphilic Polymers. *J. Am. Chem. Soc.* **2008**, *130*, 3744–3745.
- Medintz, I. L.; Berti, L.; Pons, T.; Grimes, A. F.; English, D. S.; Alessandrini, A.; Facci, P.; Mattoussi, H. A Reactive Peptidic Linker for Self-assembling Hybrid Quantum Dot–DNA Bioconjugates. *Nano Lett.* **2007**, *7*, 1741–1748.
- Fernandez-Arguelles, M. T.; Yakovlev, A.; Sperling, R. A.; Luccardini, C.; Gaillard, S.; Medel, A. S.; Mallet, J. M.; Brochon, J. C.; Feltz, A.; Oheim, M.; Parak, W. J. Synthesis and Characterization of Polymer-Coated Quantum Dots with Integrated Acceptor Dyes as FRET-Based Nanoprobes. *Nano Lett.* **2007**, *7*, 2613–2617.
- Guo, W. Z.; Li, J. J.; Wang, Y. A.; Peng, X. G. Conjugation Chemistry and Bioapplications of Semiconductor Box Nanocrystals Prepared via Dendrimer Bridging. *Chem. Mater.* **2003**, *15*, 3125–3133.
- Clapp, A. R.; Goldman, E. R.; Mattoussi, H. Capping of CdSe–ZnS Quantum Dots with DHLA and Subsequent Conjugation with Proteins. *Nat. Protoc.* **2006**, *1*, 1258–1266.
- Medintz, I. L.; Uyeda, H. T.; Goldman, E. R.; Mattoussi, H. Quantum Dot Bioconjugates for Imaging, Labelling and Sensing. *Nat. Mater.* **2005**, *4*, 435–446.
- Dabbousi, B. O.; RodriguezViejo, J.; Mikulec, F. V.; Heine, J. R.; Mattoussi, H.; Ober, R.; Jensen, K. F.; Bawendi, M. G. (CdSe)ZnS Core–Shell Quantum Dots: Synthesis and Characterization of a Size Series of Highly Luminescent Nanocrystallites. *J. Phys. Chem. B* **1997**, *101*, 9463–9475.
- Murray, C. B.; Norris, D. J.; Bawendi, M. G. Synthesis and Characterization of Nearly Monodisperse CdE (E = S, Se, Te) Semiconductor Nanocrystallites. *J. Am. Chem. Soc.* **1993**, *115*, 8706–8715.
- Förster, T. Zwischenmolekulare Energiewanderung und Fluoreszenz. *Ann. Physik* **1948**, *437*, 55–75.
- Liu, W.; Howarth, M.; Greytak, A. B.; Zheng, Y.; Nocera, D. G.; Ting, A. Y.; Bawendi, M. G. Compact Biocompatible Quantum Dots Functionalized for Cellular Imaging. *J. Am. Chem. Soc.* **2008**, *130*, 1274–1284.
- Uyeda, H. T.; Medintz, I. L.; Jaiswal, J. K.; Simon, S. M.; Mattoussi, H. Synthesis of Compact Multidentate Ligands to Prepare Stable Hydrophilic Quantum Dot Fluorophores. *J. Am. Chem. Soc.* **2005**, *127*, 3870–3878.
- Zimmer, J. P.; Kim, S. W.; Ohnishi, S.; Tanaka, E.; Frangioni, J. V.; Bawendi, M. G. Size Series of Small Indium Arsenide–Zinc Selenide Core–Shell Nanocrystals and Their Application to *In Vivo* Imaging. *J. Am. Chem. Soc.* **2006**, *128*, 2526–2527.
- Fisher, B. R.; Eisler, H. J.; Stott, N. E.; Bawendi, M. G. Emission Intensity Dependence and Single-Exponential Behavior in Single Colloidal Quantum Dot Fluorescence Lifetimes. *J. Phys. Chem. B* **2004**, *108*, 143–148.
- Hines, M. A.; Guyot-Sionnest, P. Synthesis and Characterization of Strongly Luminescing ZnS-Capped CdSe Nanocrystals. *J. Phys. Chem.* **1996**, *100*, 468–471.
- Peng, Z. A.; Peng, X. G. Formation of High-Quality CdTe, CdSe, and CdS Nanocrystals Using CdO as Precursor. *J. Am. Chem. Soc.* **2001**, *123*, 183–184.
- Jana, N. R.; Chen, Y. F.; Peng, X. G. Size- and Shape-Controlled Magnetic (Cr, Mn, Fe, Co, Ni) Oxide Nanocrystals via a Simple and General Approach. *Chem. Mater.* **2004**, *16*, 3931–3935.
- Chiefari, J.; Chong, Y. K.; Ercole, F.; Krstina, J.; Jeffery, J.; Le, T. P. T.; Mayadunne, R. T. A.; Meijs, G. F.; Moad, C. L.; Moad, G.; Rizzardo, E.; Thang, S. H. Living Free-Radical Polymerization by Reversible Addition–Fragmentation Chain Transfer: The RAFT Process. *Macromolecules* **1998**, *31*, 5559–5562.
- Sheehan, J. C.; Cruickshank, P. A.; Boshart, G. A Convenient Synthesis of Water-Soluble Carbodiimides. *J. Org. Chem.* **1961**, *26*, 2525–2528.
- McCormick, D. B. Specific Purification of Avidin by Column Chromatography on Biotin-Cellulose. *Anal. Biochem.* **1965**, *13*, 194–198.